Global Change Biology

Global Change Biology (2012) **18**, 1401–1411, doi: 10.1111/j.1365-2486.2011.02628.x

Precipitation variability and fire influence the temporal dynamics of soil CO_2 efflux in an arid grassland

RODRIGO VARGAS*, SCOTT L. COLLINS†, MICHELL L. THOMEY†, JENNIFER E. JOHNSON†, RENEE F. BROWN†, DONALD O. NATVIG† and MICHAEL T. FRIGGENS†

Departamento de Biología de la Conservación, Centro de Investigación Científica y de Educación Superior de Ensenada (CICESE), Ensenada 22860, BC Mexico, †Department of Biology, MSC03-2020, University of New Mexico, Albuquerque, NM 87131, USA

Abstract

Climate models suggest that extreme rainfall events will become more common with increased atmospheric warming. Consequently, changes in the size and frequency of rainfall will influence biophysical drivers that regulate the strength and timing of soil CO_2 efflux – a major source of terrestrial carbon flux. We used a rainfall manipulation experiment during the summer monsoon season (July–September) to vary both the size and frequency of precipitation in an arid grassland 2 years before and 2 years after a lightning-caused wildfire. Soil CO_2 efflux rates were always higher under increased rainfall event size than under increased rainfall event frequency, or ambient precipitation. Although fire reduced soil CO_2 efflux rates by nearly 70%, the overall responses to rainfall variability were consistent before and after the fire. The overall sensitivity of soil CO_2 efflux to temperature (Q_{10}) converged to 1.4, but this value differed somewhat among treatments especially before the fire. Changes in rainfall patterns resulted in differences in the periodicity of soil CO_2 efflux with strong signals at 1, 8, and 30 days. Increased rainfall event size enhanced the synchrony between photosynthetically active radiation and soil CO_2 efflux over the growing season before and after fire, suggesting a change in the temporal availability of substrate pools that regulate the temporal dynamics and magnitude of soil CO_2 efflux. We conclude that arid grasslands are capable of rapidly increasing and maintaining high soil CO_2 efflux rates in response to increased rainfall event size more than increased rainfall event frequency both before and after a fire. Therefore, the amount and pattern of multiple rain pulses over the growing season are crucial for understanding CO_2 dynamics in burned and unburned water-limited ecosystems.

Keywords: carbon cycle, climate change, disturbance, extreme pulses, grasslands, net primary production, precipitation variability, soil respiration, wavelet analysis

Received 8 November 2011; revised version received 8 November 2011 and accepted 17 November 2011

Introduction

A current challenge for climate change research is to understand how changes in the amount and pattern of precipitation affect ecosystem processes (Gerten *et al.*, 2008; Luo *et al.*, 2008). This research is especially important in aridland ecosystems because the timing and magnitude of precipitation pulses are biologically important at global (Huxman *et al.*, 2004a; Yang *et al.*, 2008) and regional scales (Sala *et al.*, 1988; Knapp & Smith, 2001). For aridland ecosystems, climate models project an increase in precipitation variability including more extreme rainfall events (Christensen *et al.*, 2007). Such changes in rainfall patterns could strongly influence the global carbon cycle (Austin *et al.*, 2004). Given that arid and semiarid environments occupy nearly 40% of terrestrial habitats (Loveland *et al.*, 2000), it is important to understand how changes in timing and magnitude of precipitation pulses will influence the biophysical mechanisms that regulate the carbon cycle at multiple temporal scales in these globally extensive ecosystems (Schimel, 2010).

Many aridlands are classified as grasslands or savannahs (Loveland *et al.*, 2000), where rainfall events determine the pulse-driven responses of these ecosystems (Noy-Meir, 1973; Sala & Lauenroth, 1982). Most research has focused on how changes in rainfall amount influence annual aboveground net primary production (NPP) (Knapp & Smith, 2001; Huxman *et al.*, 2004a; Robertson *et al.*, 2009). However, there is a need to integrate ecosystem responses (e.g., productivity, CO_2 fluxes) with multiple rain pulses over the growing season to understand the combined effects of seasonal rainfall (Ogle & Reynolds, 2004). Recent studies have explored the role of rainfall variability and extreme events in aboveground NPP and soil CO_2 efflux (i.e., carbon dioxide release from soils;

Correspondence: Rodrigo Vargas, tel. + 52 646 1750 500, fax + 52 646 1750 545, e-mail: rvargas@cicese.mx

Heisler-White *et al*., 2008, 2009; Thomey *et al*., 2011), or in combination with CO_2 fertilization to study total ecosystem carbon fluxes (Bachman *et al*., 2010).

In addition to rainfall patterns, fire is an important disturbance that influences biological (Scholes & Archer, 1997; Clark *et al*., 2002) and ecosystem processes in grasslands (Castaldi *et al*., 2010). Together, grasslands and savannahs represent more than 60% of the global terrestrial habitats that burn each year (Tansey *et al*., 2004). Fire is a critical factor for grasslands because it stimulates germination and regrowth (Parmenter, 2008), but the interaction between fire and land use change may promote ecosystem degradation and shrub encroachment in some systems (Archer *et al*., 1995; Havstad *et al*., 2006), or counteract encroachment in others (Ravi *et al*., 2010). Thus, one step to understand carbon dynamics in arid and semiarid environments is to study the response of natural and disturbed arid grasslands to changes in the timing and magnitude of rainfall. Without such information, the contribution of CO_2 from arid and semiarid environments could be grossly underestimated in regional and global carbon budgets because of improper model parameterization and structure (Schimel, 2010).

In this study we focus on the response of soil CO_2 efflux to increased precipitation variability during the summer monsoon in native, ungrazed desert grassland before and after a lightning-caused wildfire. Maximum net ecosystem exchange in this grassland occurs for only 1–2 months during the summer monsoon (Anderson-Teixeira *et al*., 2011). Thus, it is important to understand how changes in precipitation patterns and disturbances influence the biophysical drivers (e.g., temperature, water, photosynthesis) that control CO_2 emissions during this season. Based on empirical evidence (Huxman *et al*., 2004b; Knapp *et al*., 2008), it is expected that increased precipitation variability will reduce soil moisture stress and increase soil CO_2 efflux under undisturbed conditions (i.e., before a fire; Thomey *et al*., 2011). Yet, it is unclear: (a) whether the relative importance of the biophysical drivers of soil CO_2 efflux change with increasing precipitation variability and (b) how precipitation variability affects soil CO_2 efflux following disturbance (i.e., after a fire). We hypothesize that fire, as a disturbance, will overshadow the effect of increased precipitation variability and will decrease soil CO_2 efflux because of the loss of aboveground photosynthetic biomass. We used automated measurements of soil CO_2 efflux and applied time series analysis to (a) study the temporal variations of soil CO_2 efflux; (b) infer an unconfounded temperature sensitivity parameter (Q_{10}) of soil CO_2 efflux; and (c) explore the temporal synchrony between soil CO_2 efflux and photosynthetically active radiation (PAR) among treatments before and after a lightening caused wildfire.

Material and methods

Study site

We established a rainfall manipulation experiment in a long-term ungrazed grassland in the northern Chihuahuan Desert dominated by the native perennial C_4 grass, *Bouteloua eriopoda*. The study site is part of the Sevilleta Long-Term Ecological Research Project (LTER) located at the Sevilleta National Wildlife Refuge, New Mexico, United States (Muldavin *et al*., 2008; Thomey *et al*., 2011). Climate at the Sevilleta LTER site is arid to semiarid with dry cool winters and springs. Mean annual temperature is 13.2 °C with an average low of 1.6 °C in January and a high of 25.1 °C in July. From 1999 to 2008, aboveground NPP at the study site ranged from 17 to 180 g $m^{-2}yr^{-1}$ (Muldavin *et al*., 2008; Xia *et al*., 2010). Annual precipitation is highly variable within and between years (Pennington & Collins, 2007), averaging approximately 250 mm with 60% falling during the summer monsoon season (July–September). More information about the Sevilleta LTER Project can be found at http://sev.lternet.edu/.

Experimental design

The first part of the experiment (i.e., prefire) occurred during the summer monsoon seasons of 2007 and 2008. In the first week of August of 2009, an intense lightning-caused wildfire consumed the experimental plots, including the sensor instrumentation, although rainfall treatments continued throughout the 2009 monsoon season. The second part of the experiment (i.e., postfire) was resumed for the summer monsoon seasons of 2010 and 2011 after the instrumentation was replaced.

For all summer monsoon seasons (prefire and postfire), we manipulated rainfall event size and frequency using a random, replicated experimental design consisting of thirteen 8 m × 13 m plots (Thomey *et al*., 2011). Reference plots received only ambient precipitation ($n = 3$). Two rainfall treatments ($n = 5$) were applied each year throughout each monsoon season: (1) ambient rainfall plus one 20 mm rain event each month (i.e., increased rainfall event size) and (2) ambient rainfall plus four 5 mm rain events each month (i.e., increased rainfall event frequency). Thus, we added the same amount of precipitation (20 mm) per month over the monsoon season, but we varied the size (20 and 5 mm) and frequency (monthly vs. weekly) of applied precipitation events. Rainfall variability was increased without imposing unrealistic extreme rainfall events (Christensen *et al*., 2007). The overall precipitation added per monsoon season was 60 mm equivalent to an increase of ~40% over an average year (long-term monsoon mean ~150 mm). The 20 mm rainfall events simulated more extreme precipitation events, and the 5 mm events represented average precipitation inputs at the study site. On average, 71.3% of the precipitation events are ≤ 5 mm and 11.6% are between 10 and 20 mm (1988–2008; see http://sev.lternet.edu/).

Net primary production

Total NPP was estimated as the sum of aboveground and belowground NPP. Aboveground NPP was measured in two 1 m^2 subplots permanently located within each plot. Aboveground NPP measurements were recorded in the spring (at the start of the growing season) and again in fall (when perennial grasses had reached peak biomass). For every subplot, the biomass was determined from cover and height size classes based on weight-to-volume regressions developed by harvesting various sizes of each species from adjacent areas following Muldavin *et al.* (2008). A positive change in green biomass from one season to the next in each subplot was used as a measure of aboveground NPP. Belowground NPP was measured using root in-growth cores (Milchunas *et al.*, 2005). Briefly, the outer diameter of each root in-growth core was 20.3 cm and the inner diameter 15.2 cm and each core was 30 cm deep. Each root in-growth core was filled with root free soil from the study site. We installed 20 root in-growth cores in a site adjacent to the experimental plots that represented the reference treatments under ambient precipitation conditions. Belowground production did not differ between burned and unburned sites in 2010 (S. Burnett and S.L. Collins, unpublished results) allowing us to extrapolate belowground production prefire and postfire. We measured a mean belowground NPP of 450 g m^{-2} yr^{-1} (0–30 cm depth) and a mean aboveground NPP of 199 g m^{-2} yr^{-1} (Xia *et al.*, 2010) giving a mean ratio of 2.26.

Soil microenvironmental measurements

Nearly 8 months before the start of the experiment in 2007, soil sensor nodes were installed at all reference and treatment plots to ensure soil equilibration after installation (total of 13 instrumented plots). Each sensor node consisted of soil temperature, soil moisture, and soil CO_2 sensors placed under the canopy of *B. eriopoda* at three depths (2, 8, and 16 cm) as described previously (Thomey *et al.*, 2011). In addition, PAR (LI190SB-LC, LI-COR, Lincoln, NE, USA) was measured continuously at 30 min intervals at the field site throughout the duration of the study. Soil temperature (Ts) and soil water content (θ) were also measured at 30 min intervals with ECH_2O soil sensors (EC-TM Decagon Devices Inc., Pullman, WA, USA). Soil CO_2 concentration was continuously measured at 30 min intervals with Vaisala CARBOCAP CO_2 sensors (GMM222, Vaisala, Helsinki, Finland). Values of CO_2 concentration were corrected for temperature and pressure using the ideal gas law according to the manufacturer. We calculated soil respiration using the flux-gradient method as described previously for the study site (Vargas *et al.*, 2010a). Briefly, we used Fick's law of diffusion where the diffusivity of CO_2 was corrected for temperature and pressure (Jones, 1992) and calculated as a function of soil moisture, soil porosity, and soil texture (Moldrup *et al.*, 1999). Soil porosity was 0.43 m^3 m^{-3} and bulk density was 1.51 g cm^{-3}. Soils are Typic Haplargids derived from piedmont alluvium. Soil texture in the upper 20 cm is 68% sand, 22% silt, and 10% clay, with 2% calcium carbonate (Kieft *et al.*, 1998).

We calculated the relative available soil water (θ_r), and we considered that the ecosystem was under stress if the value dropped below a threshold of 0.4 as assumed in previous studies (Bernier *et al.*, 2002; Granier *et al.*, 2007). Briefly, θ_r was calculated from soil water content as follows:

$$\theta_r = \frac{\theta - \theta_w}{\theta_{fc} - \theta_w}, \quad (1)$$

where θ is the 2–16 cm average soil water content, θ_w is soil water content at permanent wilting point, and θ_{fc} represents water content and field capacity. We used soil water retention curves obtained for different soils at the Sevilleta LTER site to get field capacity and wilting point water content. Second, we calculated the intensity of the stress (I_s) (Granier *et al.*, 2007) as follows:

$$I_s = \Sigma \max\left[0, \frac{0.4 - \theta_r}{0.4}\right], \quad (2)$$

which is dimensionless and ranges between 0 (no stress) and 83 (soil water reserve totally depleted during the average length of a monsoon season).

Data analysis

Results before and after fire (prefire years 2007 and 2008; postfire years 2010 and 2011) were analyzed separately to test for the effect of treatment precipitation variability (i.e., ambient, small pulses, large pulses). Data were transformed to meet assumptions of analysis of variance (ANOVA) and analyzed using a single-factor general linear model. Significant treatment effects were followed by multiple comparisons using LS Means for unbalanced designs.

We used wavelet analysis as a time series technique that has been widely applied in the geosciences (Torrence & Compo, 1998) and for soil CO_2 efflux research (Vargas *et al.*, 2010b, 2011a). This technique is used to quantify the spectral characteristics of time series that may be nonstationary and heteroscedastic. Wavelet global power spectra were computed using MATLAB 2009a using the Morlet wavelet basis function as suggested by previous studies (Torrence & Compo, 1998; Torrence & Webster, 1999). The global wavelet power spectrum was calculated for (a) the original time series of soil CO_2 efflux for each plot and treatment and (b) the temperature detrended time series soil CO_2 efflux for each plot and treatment. Finally, we calculated the mean of the global power spectrum for each treatment for both soil CO_2 efflux measurements, and the temperature detrended soil CO_2 efflux for prefire and postfire.

The temperature detrended time series soil CO_2 effluxes were calculated from hourly averages by fitting independent regressions for each day with the form:

$$Rs_{td} = Rs_n - (\beta_0 * \exp^{(\beta_1 * Ts_n)}), \quad (3)$$

where Rs_{td} is the detrended time series soil CO_2 efflux, Rs_n is the measured soil CO_2 efflux for day n (24 measurements per day), Ts_n is the measured temperature at the 8 cm depth (depth of maximum correlation with soil CO_2 efflux) during the same day n, and β_0 and β_1 are constants calculated for each

day n. Therefore, for each day (or 24 measurements) an individual curve was fitted to detrend the data. This step is important to remove autocorrelations between soil CO_2 efflux and soil temperature as both time series are regulated by solar radiation and could lead to improper interpretations of temporal correlations (Vargas *et al.*, 2011a).

We used the results of the wavelet analysis for the original time series of soil CO_2 efflux to calculate unconfounded temperature sensitivities of soil CO_2 efflux (Q_{10hf}) for all treatments before and after the fire. Unconfounded Q_{10} values are challenging to calculate due to potential effects of changes in soil water content (Davidson & Janssens, 2006). Thus, we report Q_{10hf} derived from high-frequency (i.e., 0.5–3 day time periods) subsignals of soil CO_2 efflux decomposed using wavelet analysis. This analysis has similar theoretical bases for time series frequency decomposition to identify an unconfounded Q_{10} value as described by the SCAPE method (Mahecha *et al.*, 2010).

Finally, we used wavelet coherence analysis, to study the temporal synchrony between two time series (Vargas *et al.*, 2010b). The two time series analyzed were temperature detrended time series soil CO_2 efflux (see Eqn 3) and PAR. Wavelet coherence analysis can be thought of as the local correlation between two time series. Importantly, the wavelet coherence analysis finds regions in frequency space where two time series co-vary but do not necessarily have high common power (Grinsted *et al.*, 2004). The statistical significance (5% significance level) of common power between two time series was assessed within the cone of influence of the wavelet coherence analysis using Monte Carlo simulations (Grinsted *et al.*, 2004). The cone of influence is the region in which the wavelet transform suffers from edge effects because of incomplete time-locality across frequencies (Torrence & Compo, 1998), thus the results have to be interpreted cautiously. Before wavelet coherence analysis was performed, the time series were normalized to a mean of zero and a variance of one. Detailed reviews on the application and theory of wavelet analysis can be found in Farge (1992), Torrence & Compo (1998), and Grinsted *et al.* (2004).

Results

In 2007, reference plots received 92.2 mm of precipitation (ambient only), and treatment plots received a total of 152.2 mm of rainfall (ambient + applied), representing nearly 65% more precipitation (Fig. 1a). In 2008, reference plots received 179.6 mm of precipitation (ambient only), and treatment plots received a total of 239.6 mm of rainfall (ambient + applied), representing nearly 33% more precipitation (Fig. 1b). The summer monsoon season of 2010 represented a dry year where the reference plots received 33 mm of precipitation (ambient only) and the treatment plots received a total of 93 mm of rainfall (ambient + applied), representing nearly 180% more precipitation when compared with the reference plots (Fig. 1c). Finally, in 2011 reference

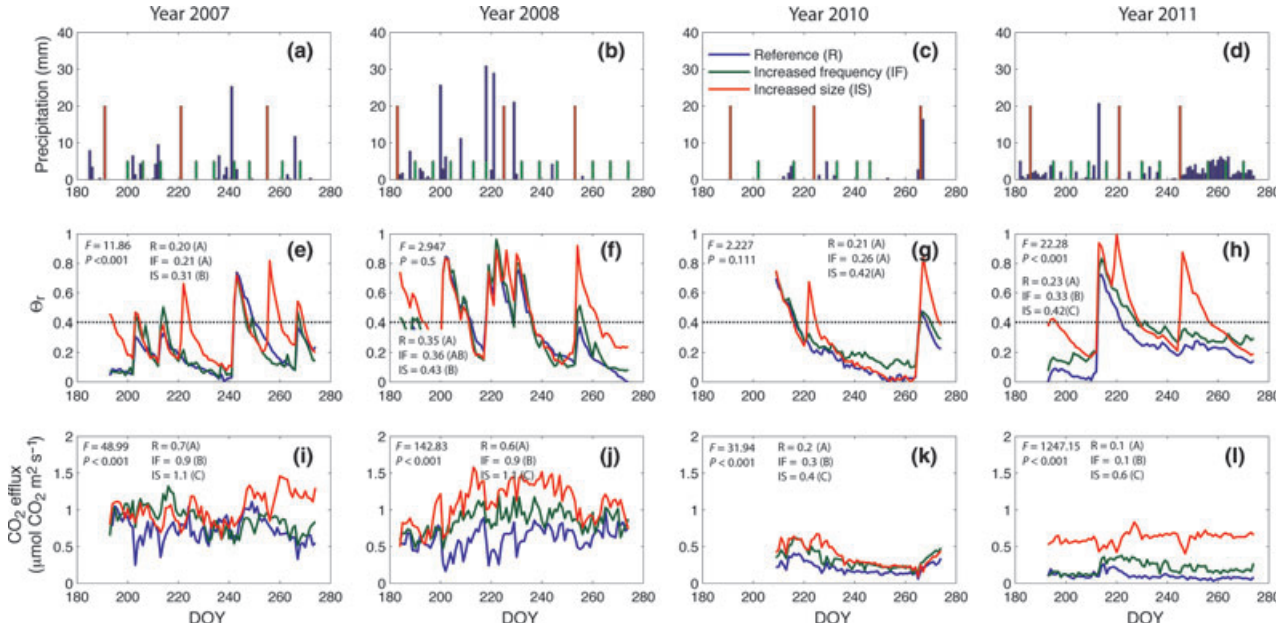

Fig. 1 Time series for prefire (July–September 2007 and 2008) and postfire (July–September 2010 and 2011) environmental variables in the monsoon rainfall manipulation experiment. Daily means are shown for rainfall (a–d), relative extractable soil water (θ_r; e–h), and soil CO_2 efflux (i–l). The dashed lines in e–h represent the water stress threshold (Granier *et al.*, 2007). Blue, ambient precipitation (n = 3); green, increased small rainfall event frequency (n = 5; ambient plus 5 mm weekly); red, increased large rainfall event size (n = 5; ambient plus 20 mm per month). Different capital letters in parenthesis denote significant differences between treatments. DOY = day of year.

plots received 152.7 mm of precipitation (ambient only), and treatment plots received a total of 212.7 mm of rainfall (ambient + applied), representing nearly 39% more precipitation (Fig. 1d).

Increased rainfall event size raised θ_r significantly over the reference and increased rainfall event frequency plots before the fire and for the year 2011 after the fire (Fig. 1e–h). No significant differences in daily θ_r occurred among treatments during the dry postfire year 2010 (Fig. 1g). Increased rainfall event size was more effective than increased rainfall event frequency in reducing the intensity of drought stress (I_s) both before and after the fire (Fig. 2).

There were no significant differences in NPP between the treatments before the fire (year 2007 mean 566 g m^{-2}, year 2008 mean 413 g m^{-2}; Fig. 2a) or after the fire (year 2010 mean 134 g m^{-2}, year 2011 mean 81 g m^{-2}; Fig. 2b). After the fire, on average, we observed a reduction in NPP of ~74% under increased rainfall event size, ~79% under increased rainfall event frequency, and ~80% in reference rainfall plots, although results varied between years (Fig. 2).

We found significantly higher prefire soil CO_2 efflux rates than postfire rates (Fig. 1i–l). Losses during the monsoon season from increased rainfall event size (up to 105 g C m^{-2}) and increased rainfall event frequency (up to 82 g C m^{-2}) were higher than those from reference plots (up to 63 g C m^{-2}) before the fire (Fig. 1i–j and Fig. 3a). Similarly, losses from increased rainfall event size (up to 52 g C m^{-2}) and increased rainfall event frequency (up to 22 g C m^{-2}) were higher than those from reference plots (up to 14 g C m^{-2}) after the fire (Fig. 1k–l and Fig. 3b). After fire, on average, we observed a reduction in soil CO_2 efflux of ~60% under increased rainfall event size, ~74% under increased rainfall event frequency, and ~80% in reference rainfall plots, although results varied between years (Fig. 3).

To explore the drivers of soil CO_2 efflux, we first tested for treatment effects on temperature sensitivity. We calculated an unconfounded parameter (Q_{10hf}) based on time frequency decomposition and found significant differences in Q_{10hf} between treatments before the fire, but with an overall mean value of 1.4 (Fig. 4a). These results showed an increase in Q_{10hf} under increased rainfall event size before the fire. In contrast, after the fire, we did not find significant differences in Q_{10hf} between treatments for 2010, and Q_{10hf} was higher only under increased rainfall event size during 2011. Similarly, the overall mean value of Q_{10hf} after the fire was 1.4 (Fig. 4b).

Importantly, daily soil temperature was not significantly different between treatments at any soil depth (between 2 and 16 cm) for both prefire and postfire (data not shown). Before the fire, differences in soil CO_2 efflux rates between treatments appear to be a function of soil moisture and changes in temperature sensitivity. After the fire, the overall reduction in soil CO_2 efflux rates appears to be controlled by NPP, but differences between treatments were a function of soil moisture in 2010, and soil moisture and temperature sensitivity in 2011.

We explored the spectral properties of the time series of soil CO_2 efflux, and we present the combined results for prefire or postfire for simplification because results were consistent among years (Fig. 5). The global wavelet power spectrums of measured soil CO_2 efflux at our experimental plots showed strong periodicities at 1 day and >10 days, but these peaks varied according to treatment. Increased rainfall event size showed stronger periodicities than increased rainfall event frequency

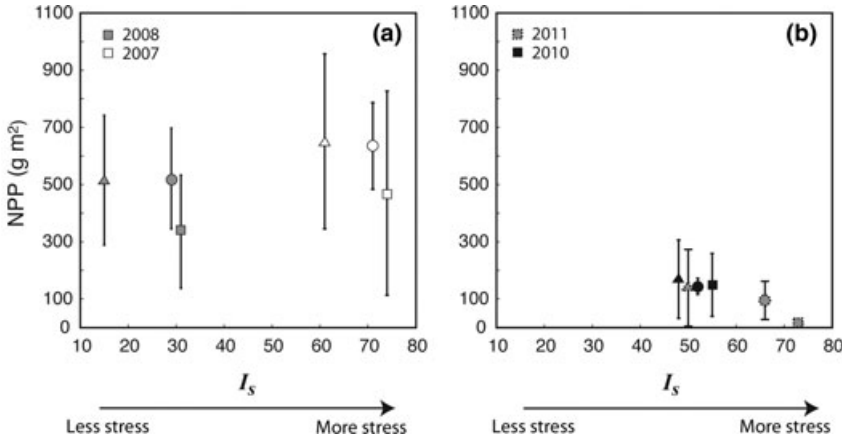

Fig. 2 Relationship between seasonal sums of net primary production (NPP) for (a) prefire or (b) postfire, and the intensity of water stress (I_s) during the monsoon rainfall season (July–September). Increased large rainfall event size (triangles), increased small rainfall event frequency (circles), and ambient precipitation (squares). Error bars represent ± 95% confidence intervals.

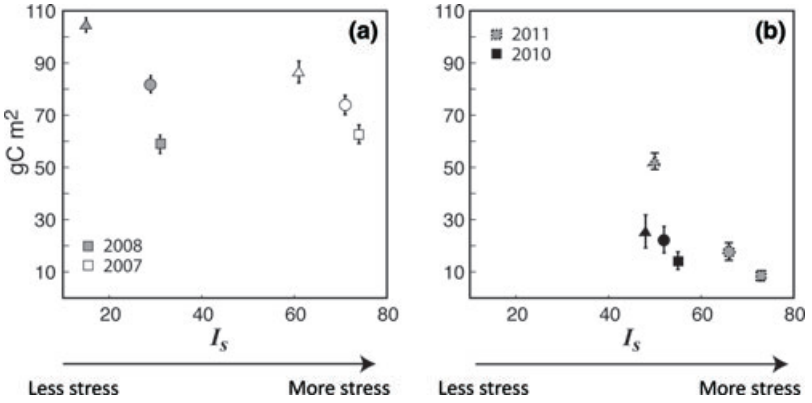

Fig. 3 Relationship between seasonal sums of soil CO_2 efflux for (a) prefire or (b) postfire, and the intensity of water stress (I_s) in the monsoon rainfall season (July–September). Increased large rainfall event size (triangles), increased small rainfall event frequency (circles), and ambient precipitation (squares). Error bars represent ± 95% confidence intervals.

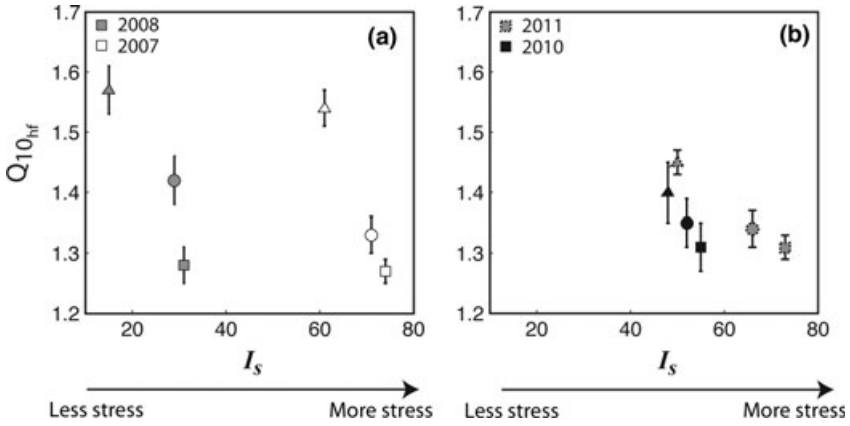

Fig. 4 Relationship between temperature sensitivity of soil CO_2 efflux (Q_{10hf}) and intensity of water stress (I_s) for (a) prefire and (b) postfire in the monsoon rainfall season (July–September). Increased large rainfall event size (triangles), increased small rainfall event frequency (circles), and ambient precipitation (squares). Error bars represent ± 95% confidence intervals.

and reference plots before the fire (Fig. 5a). In contrast, increased rainfall event frequency resulted in stronger periodicities after the fire (Fig. 5b). Temperature detrended soil CO_2 efflux showed a prominent 1 day periodicity in all rainfall treatments before and after the fire (Fig. 5c, d).

Based on the global wavelet power spectrums temperature alone could not explain all of the variability in soil CO_2 efflux (Fig. 5c, d). Therefore, we applied wavelet coherence analysis on the detrended time series of soil CO_2 efflux and PAR, which has been used as a surrogate for photosynthesis (Adams *et al.*, 2004; Liu *et al.*, 2006). Continuous measurements of photosynthesis for each treatment do not exist. Similarly to the global power spectrums, we present the combined results for simplification because results were consistent among years. Our results show a consistent and marked contrast in the periodicity and temporal coherence between these two variables among treatments (Fig. 6). Overall we observed a strong coherence at the 1 day period across treatments (i.e., more days where diel fluctuations in PAR are in synchrony with fluctuations in soil CO_2 efflux represented by the red areas in Fig. 6). Our results show that the consistency of the temporal synchrony between soil CO_2 efflux and PAR (at the 1 day period) was lowest under ambient precipitation, followed by increased rainfall event frequency, and reaching the highest consistency under increased rainfall event size. In other words, under increased rainfall event size, the temporal synchrony between soil CO_2 efflux and PAR (at the 1 day period) was the highest as represented by the red areas in Fig. 6. Differences in the synchrony of soil CO_2 efflux between treatments were most evident before the fire (Fig. 6a–c). After the fire, the synchrony appeared to be stronger in all treatments (Fig. 6d–f), when compared with prefire results (Fig. 6a–c), but the synchrony remained highest under increased rainfall event size.

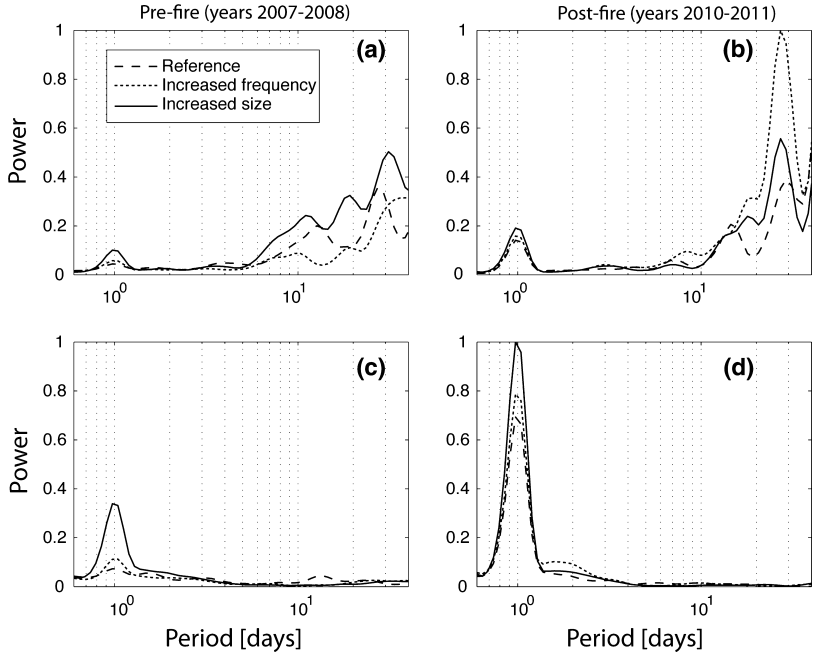

Fig. 5 Mean global wavelet power spectrum of soil CO_2 efflux in a monsoon rainfall season (July–September) for prefire (average for years 2007–2008) and postfire (average for years 2010–2011). Mean global wavelet power spectrum of soil CO_2 efflux signals (a–b), and temperature detrended soil CO_2 efflux signals (c–d) representing the variability of soil CO_2 efflux that is not explained by soil temperature.

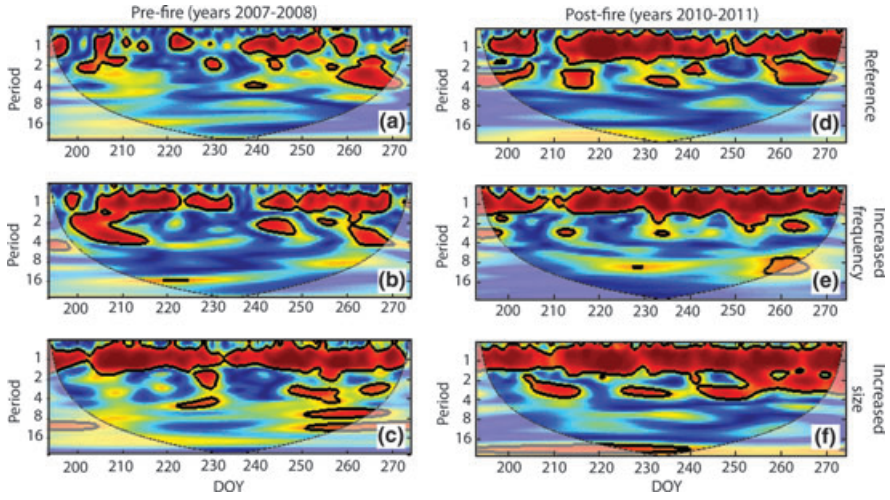

Fig. 6 Wavelet coherence analysis between temperature detrended soil CO_2 efflux and photosynthetically active radiation. The graphs represent the wavelet coherence from the monsoon rainfall season (July–September) during prefire (years 2007–2008; a–c) and postfire (years 2010–2011; d–f). The color codes for power values in graphs are from dark blue (low values of coherence) to dark red (high coherence). Black contour lines around red areas represent 5% significance level. DOY = day of year.

Discussion

Our results provide experimental evidence that increased rainfall event size resulted in high soil CO_2 efflux before and after a natural disturbance relative to increased rainfall event frequency treatments. These results have several implications. First, changes in rainfall variability can rapidly alter carbon dynamics independent of changes in total rainfall, but are highly dependent on size and frequency of rainfall events that decrease soil water stress (Huxman *et al.*, 2004b). Second, contrary to our expectations, the effects of changes

in the size and frequency of precipitation on soil CO_2 efflux were consistent before and after fire, but not for NPP response. Third, higher soil CO_2 efflux emissions were not only a result of higher temperature sensitivity (Q_{10}), but likely an enhanced temporal availability of substrate pools controlled by processes explained by temperature acting at time scales >10 days, and drivers controlled by light acting on a 24 h cycle (i.e., 1 day). Thus, our results suggest that the amount and pattern of multiple rain pulses over the growing season is important for understanding CO_2 dynamics in burned and unburned water-limited grasslands.

Our results contrast with those from mesic grasslands where an increase in rainfall variability is associated with a decrease in aboveground NPP (Heisler-White *et al.*, 2009) and soil CO_2 efflux (Harper *et al.*, 2005). The effect of growing season water pulses is critical for aboveground NPP in aridland ecosystems (Reynolds *et al.*, 2004; Collins *et al.*, 2008), as wetting depth could allow roots to utilize soil moisture in the upper (reference and increased rainfall event frequency plots) and deeper soil layers (increased rainfall event size plots) leading to increased rates of aboveground NPP of the dominant grass, *B. eriopoda* (Thomey *et al.*, 2011). After an intense wildfire, we observed that the treatments did not influence NPP suggesting that grasses did not recover sufficient aboveground biomass and leaf area to take advantage of the reduced water stress. This result shows an apparent decoupling between postfire NPP and soil CO_2 efflux rates that could be thought as a potential change in the sources of CO_2 production after fire (Czimczik *et al.*, 2006).

Before the fire, we observed up to 105 g C m^{-2} emissions from soils during the monsoon season in plots receiving a small number of large rainfall events. This rate is lower than the global annual mean of ecosystem respiration 868 g C m^{-2} yr^{-1} reported for grasslands within FLUXNET (i.e., the global consortium of eddy covariance towers; Baldocchi, 2008). Despite the reduction in efflux rates after the fire, our results show that arid grasslands are capable of rapidly increasing and maintaining higher soil CO_2 efflux rates during the growing season in response to large rainfall events that decrease the intensity of water stress.

It is known that carbon emissions from arid grasslands are often limited by moisture during the warm growing season, but that temperature plays an important role once moisture stress is reduced (Cable *et al.*, 2010; Anderson-Teixeira *et al.*, 2011). Furthermore, for proper model parameterization, it is critical to test if the temperature sensitivity for soil CO_2 efflux changes under climate change scenarios and different disturbances. Our results show that a reduction in moisture stress was associated with higher temperature sensitivity, except for the year following the fire (year 2010). This is likely a result of low microbial and plant activity following the fire event (Herrera *et al.*, 2011). Importantly, we found an overall Q_{10hf} of nearly 1.4 among treatments and years, which is consistent with values reported for arid grasslands (Cable *et al.*, 2010) and the global Q_{10} across different ecosystems (Bond-Lamberty & Thomson, 2010; Mahecha *et al.*, 2010). Our results are comparable to those of undisturbed mesic grasslands where changes in precipitation variability resulted in different Q_{10} values (Harper *et al.*, 2005). Our results are based on continuous measurements and time frequency decomposition to calculate an unconfounded Q_{10}, and previous observations should be revised for disturbed and undisturbed mesic grasslands based on this approach.

Results from our study show that the temporal dynamics of soil CO_2 efflux are modified by changes in size and frequency of rainfall as shown by the global wavelet power spectrum (Fig. 5). Because higher soil CO_2 efflux rates were not only a result of changes in Q_{10hf} an alternative explanation is an increase in the temporal availability of different substrate pools for soil CO_2 efflux as water stress decreases. Direct measurement of substrate pools for soil CO_2 efflux could be inferred using radiocarbon (Czimczik *et al.*, 2006; Vargas *et al.*, 2011b), but this technique is expensive, time consuming and cannot be done continuously with current technology. We propose that the information contained in a time series of CO_2 efflux measurements could provide insights into the relative importance of various drivers (Fig. 7). For example, the global wavelet power spectrum reveals important periods at 1, 8, and 30 days (Fig. 7c), which are associated with high-, medium-, and low-frequency signals, respectively (Fig. 7b). It is known that high levels of β-glucosidases and phenoloxidases occur in Sevilleta soils (Stursova *et al.*, 2006; Zeglin *et al.*, 2007) suggesting significant microbial use of both labile and recalcitrant soil carbon sources. Thus, information contained in high-frequency signals may be associated with fluxes derived from sources with high turnover rates. In contrast, low-frequency signals may be associated with fluxes derived from sources with low turnover rates and where carbon may have longer residence time (Fig. 7b).

We used wavelet coherence analysis to explore drivers that could control sources with high turnover rates by analyzing the temperature detrended time series of CO_2 efflux and PAR, which have a strong 1 day synchrony (Fig. 5c, d). Recent studies have noted a clear and rapid link between photosynthesis and soil CO_2 efflux for arid (Carbone *et al.*, 2011; Yan *et al.*, 2011) and mesic grasslands (Wan & Luo, 2003; Bahn *et al.*, 2009;

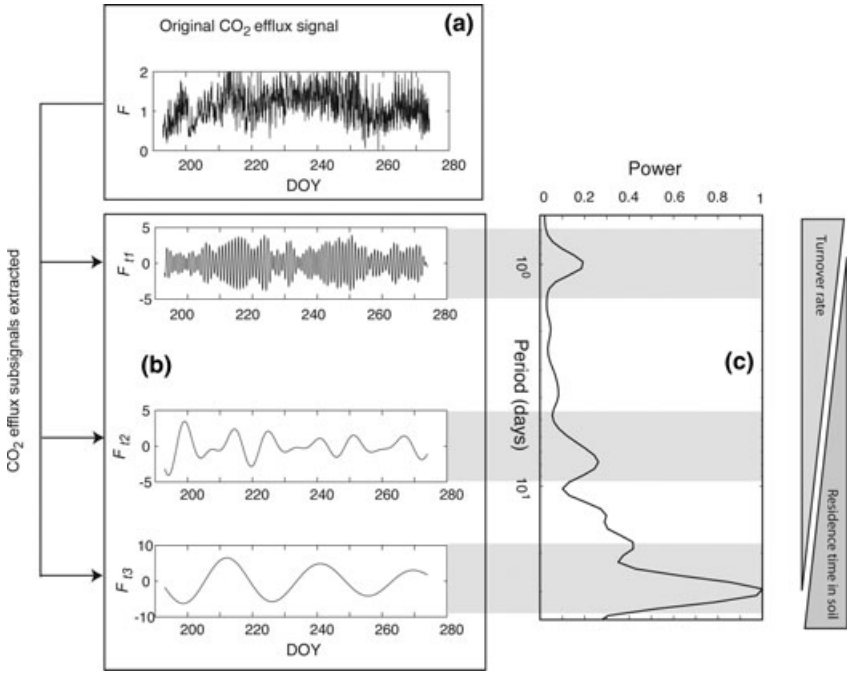

Fig. 7 Time frequency decomposition of the original soil CO_2 efflux signal (a) into subsignals (b) (modified after Mahecha *et al.*, 2010). Extracted subsignals represent important periods identified by the global wavelet power spectrum (c). High-frequency subsignals of soil CO_2 efflux (F_{t1}) are likely associated with processes with fast turnover rates and where carbon has a low residence time in the soil. Low-frequency subsignals of soil CO_2 efflux (F_{t3}) are likely associated with processes with low turnover rates and where carbon has a longer residence time in the soil.

Vargas *et al.*, 2011a). Our results support these studies by showing a strong temporal correlation between the temperature detrended time series of CO_2 efflux and PAR, which represents the potential diel oscillations of photosynthesis in the frequency domain. Our results show that the temporal relationship between PAR and soil CO_2 efflux can be modified by changes in frequency and size of rainfall events. We postulate that this temporal change likely enhances a substrate pool via rapid transfer of current photosynthates belowground resulting in high autotrophic and heterotrophic respiration (Wan & Luo, 2003; Bahn *et al.*, 2009; Yan *et al.*, 2011). Our results show that under ambient rainfall, the synchrony between PAR and soil CO_2 efflux is not consistent with time resulting in lower soil CO_2 efflux rates. Under increased rainfall event size, the synchrony is more consistent in time resulting in higher soil CO_2 efflux rates. In other words, the number of days during the growing season where fast turnover substrate supply, potentially provided by photosynthesis, may influence soil CO_2 efflux is larger under large infrequent rainfall events as a result of prolonged soil moisture availability (Thomey *et al.*, 2011).

Our results on the effect of changes in precipitation variability on the synchrony of soil CO_2 efflux and PAR were consistent before and after fire, despite the reduction in NPP and total rainfall during the monsoon season (Fig. 6). It is not clear how disturbances influence the control of photosynthesis on soil CO_2 efflux, but we observed a stronger temporal correlation between CO_2 efflux and PAR after the wildfire (Fig. 6d–f). These results suggest that soil CO_2 potentially derived from a rapid turnover of carbohydrate from photosynthesis is more important for the overall soil CO_2 efflux after fire than rainfall pulses. This interpretation is supported by radiocarbon analyses from soil CO_2 efflux showing an increase in the contribution of carbon derived from recent photosynthetic products after a fire in a boreal forest (Czimczik *et al.*, 2006), but clearly more research in aridland ecosystems is needed to corroborate this interpretation in combination to precipitation events.

In conclusion, our results show that arid grasslands are capable of rapidly increasing and maintaining higher soil CO_2 efflux rates during the growing season in response to large infrequent rainfall events that decrease the intensity of water stress. This pattern was consistent before and after an intense wildfire. We postulate that an increase in soil CO_2 efflux is likely a result of enhanced temporal availability of low turnover rate substrate pools controlled by temperature at lower frequencies (>10 days) and high turnover rate substrate pools likely controlled by photosynthesis

substrate supply at higher frequencies (~1 day). A decrease in soil water stress is likely to change the temperature sensitivity (Q_{10}) of soil CO_2 efflux, but the overall Q_{10} reported in this experiment is similar to the global value of 1.4. A decrease in soil water stress increased the temporal synchrony between PAR and soil CO_2 efflux. This temporal synchrony may be more important for soil CO_2 efflux after a fire event by maintaining a high turnover rate through photosynthesis substrate supply. Given the large extent of arid and semiarid environments (Loveland *et al*., 2000) and the potential increase in extreme rainfall events (Kharin *et al*., 2007; Allan & Soden, 2008), it is important that empirical studies and process-based models explore the sensitivity of carbon fluxes to rainfall pulses across an arid to mesic environmental gradient. These experiments are crucial for both proper model parameterization and better estimates of carbon dynamics in aridland ecosystems. Finally, long-term observations are needed to clearly elucidate how disturbances control ecosystem processes, as postdisturbances trajectories are dependent on postdisturbance conditions and climate variability.

Acknowledgements

David Schimel, Dennis Baldocchi, Matteo Detto, and Stephen Smith provided valuable comments on previous versions of our manuscript. Funding was provided by the University of New Mexico and grants from the National Science Foundation for Long-Term Ecological Research (DEB-0620482) and the US Department of Energy's Office of Science (BER) through the Western Regional Center of the National Institute for Climatic Change Research. R. V. was funded by the Consejo Nacional de Ciencia y Tecnología (Repatriación and Ciencia Básica Grants) while writing this manuscript.

References

Adams B, White A, Lenton TM (2004) An analysis of some diverse approaches to modelling terrestrial net primary productivity. *Ecological Modelling*, **177**, 353–391.

Allan RP, Soden BJ (2008) Atmospheric warming and the amplification of precipitation extremes. *Science*, **321**, 1481–1484.

Anderson-Teixeira KJ, Delong JP, Fox AM, Brese DA, Litvak ME (2011) Differential responses of production and respiration to temperature and moisture drive the carbon balance across a climatic gradient in New Mexico. *Global Change Biology*, **17**, 410–424.

Archer S, Schimel DS, Holland EA (1995) Mechanisms of shrubland expansion: land use, climate or CO_2? *Climatic Change*, **29**, 91–99.

Austin AT, Yahdjian L, Stark JM *et al*. (2004) Water pulses and biogeochemical cycles in arid and semiarid ecosystems. *Oecologia*, **141**, 221–235.

Bachman S, Heisler-White JL, Pendall E, Williams DG, Morgan JA, Newcomb J (2010) Elevated carbon dioxide alters impacts of precipitation pulses on ecosystem photosynthesis and respiration in a semi-arid grassland. *Oecologia*, **162**, 791–802.

Bahn M, Schmitt M, Siegwolf R, Richter A, Bruggemann N (2009) Does photosynthesis affect grassland soil-respired CO_2 and its carbon isotope composition on a diurnal timescale? *New Phytologist*, **182**, 451–460.

Baldocchi D (2008) Breathing of the terrestrial biosphere: lessons learned from a global network of carbon dioxide flux measurement systems. *Australian Journal of Botany*, **56**, 1–26.

Bernier PY, Breda N, Granier A, Raulier F, Mathieu F (2002) Validation of a canopy gas exchange model and derivation of a soil water modifier for transpiration for sugar maple (Acer saccharum Marsh.) using sap flow density measurements. *Forest Ecology and Management*, **163**, 185–196.

Bond-Lamberty B, Thomson A (2010) Temperature-associated increases in the global soil respiration record. *Nature*, **464**, 579–582.

Cable JM, Ogle K, Lucas RW *et al*. (2010) The temperature responses of soil respiration in deserts: a seven desert synthesis. *Biogeochemistry*, **103**, 71–90.

Carbone MS, Still CJ, Ambrose AR *et al*. (2011) Seasonal and episodic moisture controls on plant and microbial contributions to soil respiration. *Oecologia*, **167**, 265–278.

Castaldi S, De Grandcourt A, Rasile A, Skiba U, Valentini R (2010) CO_2, CH_4 and N_2O fluxes from soil of a burned grassland in Central Africa. *Biogeosciences*, **7**, 3459–3471.

Christensen JH, Hewitson B, Busuioc A *et al*. (2007) Regional climate projections, climate change, 2007: the physical science basis. In: *Contribution of Working Group I to the Fourth Assessment Report of the Intergovernmental Panel on Climate Change* (eds Solomon S, Qin D, Manning M, Chen Z, Marquis M, Averyt KB, Tignor M, Miller HL), pp. 847–940. Cambridge University Press, Cambridge, UK and New York, NY, USA.

Clark JS, Grimm EC, Donovan JJ, Fritz SC, Engstrom DR, Almendinger JE (2002) Drought cycles and landscape responses to past aridity on prairies of the northern Great Plains, USA. *Ecology*, **83**, 595–601.

Collins SL, Sinsabaugh RL, Crenshaw C, Green L, Porras-Alfaro A, Stursova M, Zeglin LH (2008) Pulse dynamics and microbial processes in aridland ecosystems. *Journal of Ecology*, **96**, 413–420.

Czimczik CI, Trumbore SE, Carbone MS, Winston GC (2006) Changing sources of soil respiration with time since fire in a boreal forest. *Global Change Biology*, **12**, 957–971.

Davidson EA, Janssens IA (2006) Temperature sensitivity of soil carbon decomposition and feedbacks to climate change. *Nature*, **440**, 165–173.

Farge M (1992) Wavelet transforms and their applications to turbulence. *Annual Review of Fluid Mechanics*, **24**, 395–457.

Gerten D, Luo Y, Le Maire G *et al*. (2008) Modelled effects of precipitation on ecosystem carbon and water dynamics in different climatic zones. *Global Change Biology*, **14**, 2365–2379.

Granier A, Reichstein M, Breda N *et al*. (2007) Evidence for soil water control on carbon and water dynamics in European forests during the extremely dry year: 2003. *Agricultural and Forest Meteorology*, **143**, 123–145.

Grinsted A, Moore JC, Jevrejeva S (2004) Application of the cross wavelet transform and wavelet coherence to geophysical time series. *Nonlinear Processes in Geophysics*, **11**, 561–566.

Harper CW, Blair JM, Fay PA, Knapp AK, Carlisle JD (2005) Increased rainfall variability and reduced rainfall amount decreases soil CO_2 flux in a grassland ecosystem. *Global Change Biology*, **11**, 322–334.

Havstad KM, Huenneke LF, Schlesinger WH (2006) *Structure and Function of a Chihuahuan Desert Ecosystem: The Jornada Basin Long-Term Ecological Research Site*. Oxford University Press, Oxford/New York.

Heisler-White JL, Knapp AK, Kelly EF (2008) Increasing precipitation event size increases aboveground net primary productivity in a semi-arid grassland. *Oecologia*, **158**, 129–140.

Heisler-White JL, Blair JM, Kelly EF, Harmoney K, Knapp AK (2009) Contingent productivity responses to more extreme rainfall regimes across a grassland biome. *Global Change Biology*, **15**, 2894–2904.

Herrera J, Poudel R, Nebel KA, Collins SL (2011) Precipitation increases the abundance of some groups of root-associated fungal endophytes in a semiarid grassland. *Ecosphere*, **2**, Art. 50.

Huxman TE, Smith MD, Fay PA *et al*. (2004a) Convergence across biomes to a common rain-use efficiency. *Nature*, **429**, 651–654.

Huxman TE, Snyder KA, Tissue D *et al*. (2004b) Precipitation pulses and carbon fluxes in semiarid and arid ecosystems. *Oecologia*, **141**, 254–268.

Jones HG (1992) *Plants and Microclimate: A Quantitative Approach to Environmental Plant Physiology*. Cambridge University Press, New York.

Kharin VV, Zwiers FW, Zhang XB, Hegerl GC (2007) Changes in temperature and precipitation extremes in the IPCC ensemble of global coupled model simulations. *Journal of Climate*, **20**, 1419–1444.

Kieft TL, White CS, Loftin SR, Aguilar R, Craig JA, Skaar DA (1998) Temporal dynamics in soil carbon and nitrogen resources at a grassland-shrubland ecotone. *Ecology*, **79**, 671–683.

Knapp AK, Smith MD (2001) Variation among biomes in temporal dynamics of aboveground primary production. *Science*, **291**, 481–484.

Knapp AK, Beier C, Briske DD *et al*. (2008) Consequences of more extreme precipitation regimes for terrestrial ecosystems. *BioScience*, **58**, 811–821.

Liu Q, Edwards NT, Post WM, Gu L, Ledford J, Lenhart S (2006) Temperature-independent diel variation in soil respiration observed from a temperate deciduous forest. *Global Change Biology*, **12**, 2136–2145.

Loveland TR, Reed BC, Brown JF, Ohlen DO, Zhu Z, Yang L, Merchant JW (2000) Development of a global land cover characteristics database and IGBP discover from 1 km AVHRR data. *International Journal of Remote Sensing*, **21**, 1303–1330.

Luo YQ, Gerten D, Le Maire G *et al*. (2008) Modeled interactive effects of precipitation, temperature, and [CO_2] on ecosystem carbon and water dynamics in different climatic zones. *Global Change Biology*, **14**, 1986–1999.

Mahecha MD, Reichstein M, Carvalhais N *et al*. (2010) Global convergence in the temperature sensitivity of respiration at ecosystem level. *Science*, **329**, 838–840.

Milchunas DG, Mosier AR, Morgan JA, Lecain DR, King JY, Nelson JA (2005) Root production and tissue quality in a shortgrass steppe exposed to elevated CO_2: using a new ingrowth method. *Plant and Soil*, **268**, 111–122.

Moldrup P, Olesen T, Yamaguchi T, Schjonning P, Rolston DE (1999) Modeling diffusion and reaction in soils. IX. The Bucking-ham-Burdine-Campbell equation for gas diffusivity in undisturbed soil. *Soil Science*, **164**, 542–551.

Muldavin EH, Moore DI, Collins SL, Wetherill KR, Lightfoot DC (2008) Aboveground net primary production dynamics in a northern Chihuahuan Desert ecosystem. *Oecologia*, **155**, 123–132.

Noy-Meir I (1973) Desert ecosystems: environment and producers. *Annual Review of Ecology and Systematics*, **4**, 25–51.

Ogle K, Reynolds JF (2004) Plant responses to precipitation in desert ecosystems: integrating functional types, pulses, thresholds, and delays. *Oecologia*, **141**, 282–294.

Parmenter RR (2008) Long-term effects of a summer fire on desert grassland plant demographics in New Mexico. *Rangeland Ecology & Management*, **61**, 156–168.

Pennington DD, Collins SL (2007) Response of an aridland ecosystem to interannual climate variability and prolonged drought. *Landscape Ecology*, **22**, 897–910.

Ravi S, D'odorico P, Huxman TE, Collins SL (2010) Interactions between soil erosion processes and fires: implications for the dynamics of fertility islands. *Rangeland Ecology & Management*, **63**, 267–274.

Reynolds JF, Kemp PR, Ogle K, Fernandez RJ (2004) Modifying the 'pulse-reserve' paradigm for deserts of North America: precipitation pulses, soil water, and plant responses. *Oecologia*, **141**, 194–210.

Robertson TR, Bell CW, Zak JC, Tissue DT (2009) Precipitation timing and magnitude differentially affect aboveground annual net primary productivity in three perennial species in a Chihuahuan Desert grassland. *New Phytologist*, **181**, 230–242.

Sala OE, Lauenroth WK (1982) Small rainfall events: an ecological role in semi-arid regions. *Oecologia*, **53**, 301–304.

Sala OE, Parton WJ, Joyce LA, Lauenroth WK (1988) Primary production of the central grassland region of the United-States. *Ecology*, **69**, 40–45.

Schimel DS (2010) Drylands in the Earth system. *Science*, **327**, 418–419.

Scholes RJ, Archer SR (1997) Tree-grass interactions in savannas. *Annual Review of Ecology and Systematics*, **28**, 517–544.

Stursova M, Crenshaw CL, Sinsabaugh RL (2006) Microbial responses to long-term N deposition in a semiarid grassland. *Microbial Ecology*, **51**, 90–98.

Tansey K, Gregoire JM, Stroppiana D *et al*. (2004) Vegetation burning in the year 2000: global burned area estimates from SPOT VEGETATION data. *Journal of Geophysical Research-Atmospheres*, **109**, Art: D14.

Thomey ML, Collins SL, Vargas R, Johnson JE, Brown RF, Natvig DO, Friggens MT (2011) Effect of precipitation variability on net primary production and soil respiration in a Chihuahuan Desert grassland. *Global Change Biology*, **17**, 1505–1515.

Torrence C, Compo GP (1998) A practical guide to wavelet analysis. *Bulletin of the American Meteorological Society*, **79**, 61–78.

Torrence C, Webster PJ (1999) Interdecadal changes in the ENSO-monsoon system. *Journal of Climate*, **12**, 2679–2690.

Vargas R, Baldocchi DD, Allen MF *et al*. (2010a) Looking deeper into the soil: biophysical controls and seasonal lags of soil CO_2 production and efflux. *Ecological Applications*, **20**, 1569–1582.

Vargas R, Detto M, Baldocchi DD, Allen MF (2010b) Multiscale analysis of temporal variability of soil CO_2 production as influenced by weather and vegetation. *Global Change Biology*, **16**, 1589–1605.

Vargas R, Baldocchi DD, Bahn M *et al*. (2011a) On the multi-temporal correlation between photosynthesis and soil CO_2 efflux: reconciling lags and observations. *New Phytologist*, **191**, 1006–1017.

Vargas R, Carbone MS, Reichstein M, Baldocchi DD (2011b) Frontiers and challenges in soil respiration research: from measurements to model-data integration. *Biogeochemistry*, **102**, 1–13.

Wan SQ, Luo YQ (2003) Substrate regulation of soil respiration in a tallgrass prairie: results of a clipping and shading experiment. *Global Biogeochemical Cycles*, **17**, Art: 1054.

Xia Y, Moore DI, Collins SL, Muldavin EH (2010) Aboveground production and species richness of annuals in Chihuahuan Desert grassland and shrubland plant communities. *Journal of Arid Environments*, **74**, 378–385.

Yan LM, Chen SP, Huang JH, Lin GH (2011) Water regulated effects of photosynthetic substrate supply on soil respiration in a semiarid steppe. *Global Change Biology*, **17**, 1990–2001.

Yang YH, Fang JY, Ma WH, Wang W (2008) Relationship between variability in aboveground net primary production and precipitation in global grasslands. *Geophysical Research Letters*, **35**, Art: L23710.

Zeglin LH, Stursova M, Sinsabaugh RL, Collins SL (2007) Microbial responses to nitrogen addition in three contrasting grassland ecosystems. *Oecologia*, **154**, 349–359.